YIELD AND DEPTH OF BURIAL HYDRODYNAMIC CALCULATIONS IN GRANODIORITE:IMPLICATIONS FOR THE NORTH KOREAN TEST SITE

Esteban Rougier, Christopher R. Bradley, Howard J. Patton, and Earl E. Knight

Los Alamos National Laboratory

Sponsored by the National Nuclear Security Administration

Award No. DE-AC52-06NA25396 / LA10-Source-NDD02

ABSTRACT

This paper reports on continued research toward establishing a consistent modeling framework for calculating nuclear explosions in earth materials. The model must be consistent with observed phenomena in the near-field by correctly 1) calculating the resulting explosive cavity radius for a given yield and depth of burial, 2) accounting for the correct energy deposition by partitioning it into internal (heat and plastic strain) and kinetic (e.g. radiated seismic) energy, 3) predicting the free-field displacement/velocities waveforms and 4) predicting the measured attenuation of the free-field peak velocity with distance. The model developed in the last year satisfies all of these criteria and has been exercised in the investigation of the 2009 North Korean nuclear test. The main findings reported in this paper are: a) the extension of the developed model to the analysis of scaled depth of burial and free surface effects in 2D Earth structure, and b) the improvement of the computational equation of state (EOS) for granite/granodiorite and some examples of the models self-consistency. Our study focuses on the North Korean test site and the May 2009 test. When compared to the Denny and Johnson (1991) and to the Heard and Ackerman (1967) cavity radius scaling models, the results presented in this paper show a clear preference to the statistical model developed by Denny and Johnson. In addition, comparative work between Patton (2011) and the model developed under this project provides a lower limit to the yield and depth of burial for the 2009 North Korean test. A series of sensitivity analysis comprising the variation of key material properties and the incorporation of topography is being produced at the time of writing this paper and will be presented at the conference. This extended analysis will provide additional bounds on the uncertainty for these estimates.

A strong motion hydrodynamics code was used to investigate the dependence of cavity dynamics and final cavity radius on the main material properties (Young's modulus, shear modulus, porosity, etc.). The material model developed was obtained by taking the Piledriver and the Hardhat nuclear test events as the main design references. The following features of the problem were identified when developing the material model: velocity profiles at given stations (near field), source modeling alternatives (iron pill, ideal gas, Hydses/SESAME), energy partition after the shot, peak velocity and peak displacement attenuation profiles and final cavity size as a function of the depth of burial. Previous attempts made with existing material models failed to comply with one or more of these features. The Tillotson type of equation of state combined with a shear plastic strain-dependent strength model was implemented and used to observe surface effects from various scaled depths of burial for a nuclear explosion.

The developed material model was used in a set of 2D axially symmetric simulations with a flat free surface, i.e., no topography. Given the best estimates for the material parameters and the fact that there was no evidence of surface spall at the North Korean test site after the 2009 nuclear test, the calculations place a minimum yield and depth of burial of 5.7 kilotons and 375 meters for a uniform source region. Further refinement of these numbers will only be possible by introducing a more realistic topography profile corresponding to the North Korean test site.

Report Documentation Page

Form Approved
OMB No. 0704-0188

1. REPORT DATE	2. REPORT TYPE	3. DATES COVERED
SEP 2011		**00-00-2011 to 00-00-2011**

4. TITLE AND SUBTITLE	5a. CONTRACT NUMBER
Yield and Depth of Burial Hydrodynamic Calculations in Granodiorite: Implications for the North Korean Test Site	5b. GRANT NUMBER
	5c. PROGRAM ELEMENT NUMBER
6. AUTHOR(S)	5d. PROJECT NUMBER
	5e. TASK NUMBER
	5f. WORK UNIT NUMBER
7. PERFORMING ORGANIZATION NAME(S) AND ADDRESS(ES) **Los Alamos National Laboratory,P.O. Box 1663 ,Los Alamos,NM,87545**	8. PERFORMING ORGANIZATION REPORT NUMBER
9. SPONSORING/MONITORING AGENCY NAME(S) AND ADDRESS(ES)	10. SPONSOR/MONITOR'S ACRONYM(S)
	11. SPONSOR/MONITOR'S REPORT NUMBER(S)

12. DISTRIBUTION/AVAILABILITY STATEMENT
Approved for public release; distribution unlimited

13. SUPPLEMENTARY NOTES
Published in the Proceedings of the 2011 Monitoring Research Review - Ground-Based Nuclear Explosion Monitoring Technologies, 13-15 September 2011, Tucson, AZ. Volume I. Sponsored by the Air Force Research Laboratory (AFRL) and the National Nuclear Security Administration (NNSA). U.S. Government or Federal Rights License

14. ABSTRACT

This paper reports on continued research toward establishing a consistent modeling framework for calculating nuclear explosions in earth materials. The model must be consistent with observed phenomena in the near-field by correctly 1) calculating the resulting explosive cavity radius for a given yield and depth of burial, 2) accounting for the correct energy deposition by partitioning it into internal (heat and plastic strain) and kinetic (e.g. radiated seismic) energy, 3) predicting the free-field displacement/velocities waveforms and 4) predicting the measured attenuation of the free-field peak velocity with distance. The model developed in the last year satisfies all of these criteria and has been exercised in the investigation of the 2009 North Korean nuclear test. The main findings reported in this paper are: a) the extension of the developed model to the analysis of scaled depth of burial and free surface effects in 2D Earth structure, and b) the improvement of the computational equation of state (EOS) for granite/granodiorite and some examples of the models self-consistency. Our study focuses on the North Korean test site and the May 2009 test. When compared to the Denny and Johnson (1991) and to the Heard and Ackerman (1967) cavity radius scaling models, the results presented in this paper show a clear preference to the statistical model developed by Denny and Johnson. In addition, comparative work between Patton (2011) and the model developed under this project provides a lower limit to the yield and depth of burial for the 2009 North Korean test. A series of sensitivity analysis comprising the variation of key material properties and the incorporation of topography is being produced at the time of writing this paper and will be presented at the conference. This extended analysis will provide additional bounds on the uncertainty for these estimates. A strong motion hydrodynamics code was used to investigate the dependence of cavity dynamics and final cavity radius on the main material properties (Young?s modulus, shear modulus, porosity, etc.). The material model developed was obtained by taking the Piledriver and the Hardhat nuclear test events as the main design references. The following features of the problem were identified when developing the material model: velocity profiles at given stations (near field), source modeling alternatives (iron pill, ideal gas, Hydses/SESAME), energy partition after the shot, peak velocity and peak displacement attenuation profiles and final cavity size as a function of the depth of burial. Previous attempts made with existing material models failed to comply with one or more of these features. The Tillotson type of equation of state combined with a shear plastic strain-

15. SUBJECT TERMS

16. SECURITY CLASSIFICATION OF:			17. LIMITATION OF ABSTRACT	18. NUMBER OF PAGES	19a. NAME OF RESPONSIBLE PERSON
a. REPORT	b. ABSTRACT	c. THIS PAGE			
unclassified	**unclassified**	**unclassified**	**Same as Report (SAR)**	**10**	

OBJECTIVES

Source characterization is the focus of this project. Understanding the physical basis of seismic wave generation is recognized as the key to advancing our ability to characterize the explosion source.

The first main objective of the current research is to undertake a series of computer simulations to study the evolution of the cavity radius under different conditions. This phase of computer simulations will employ LANL strong motion codes (CASH) for uniform source region structures to investigate the dependence of cavity dynamics and final radius on material properties, such as Young's and shear moduli, gas porosity, overburden (ρgh), regional stresses, etc. The calculations were done using a material having some similarity to the granodiorite that exists at the Democratic People's Republic of Korea (DPRK) test site.

The second main objective of the current work is to perform 2D axially symmetric and 3D computer simulations that will introduce sub-surface heterogeneity and free surface topography into the models. Here the focus will be to identify the impact of certain idealized source region structures on the dynamics of cavity growth and on the radiated seismic energy. These structures will be introduced into models of the source region in controlled ways in order to isolate their effects on the close-in phenomenology and to identify features in the cavity growth and seismic radiation associated with those effects.

RESEARCH ACCOMPLISHED

Introduction. A number of cavity radius (R_c) scaling models have been developed since the beginning of the underground nuclear testing era. The most widely used by the seismology community are the ones developed by Denny and Johnson (1991) (DJ91) and by Heard and Ackerman (1967) (HA67). At nominal depth of burials (DoBs) the predictions of these two scaling relations are in quite fair agreement between them and also with experimental data. However when the DoB is increased beyond the nominal values, the predictions steadily diverge and differ by 51% at 1000 scaled meters for a granite medium. As a result, yield estimates made for the 25 May 2009 North Korean test based on seismic magnitudes depend strongly on the chosen scaling model. Hydrodynamic calculations involving realistic material response models offer a viable alternative to characterize R_c scaling for a range of scaled DoB (SDoB) where limited data from past nuclear tests exist. Results of such calculations are presented for a granite medium with a material response validated by modeling four phenomenological criteria for past nuclear tests in granite (free field velocity waveforms, energy partitioning into the seismic wavefield, velocity attenuation profiles, and measured R_c). The numerical results presented in this paper unambiguously favor the R_c scaling model of DJ91. Lower bounds on yield and DoB of the North Korean test are constrained by predictions of an SDoB threshold for free surface damage from 2-D simulations since no such reported damage was observed for this test. The DJ91 model indicates the minimum yield and DoB for the 25 May 2009 North Korean test is 5.7 kilotons and 375 m.

Background. Traditional approaches to seismic yield estimation depend heavily on empiricism and on calibration of path effects for test sites around the world. Even the best efforts to calibrate test sites were not enough to monitor compliance with the Threshold Test Ban Treaty (TTBT), and treaty protocols had to be re-negotiated to allow for Joint Verification Experiments (JVEs) on both U.S. and Soviet test sites (Douglas and Marshall, 1996). For broad area monitoring purposes, yield estimation is further challenged because empirical approaches are plagued by inadequate calibration data and by uncertainties about the source emplacement which may not conform to standard nuclear containment practices on which seismic-derived empirical methods are based.

Results of the JVEs validated seismologists' claims of the existence of a test site body wave magnitude (m_b) bias between U. S. and the former Soviet Union test sites in Nevada and Semipalatinsk. The use of remotely-collected seismic data to calibrate test sites was vindicated, and it was shown that calibration issues can be overcome even for broad-area monitoring applications. However, the concerns about non-standard containment practices persist and need to be addressed as experience with the DPRK tests shows.

A plot of yield vs. DoB tradeoff curves (TOCs) for the 25 May 2009 DPRK test is shown in Figure 1. The TOCs are based on empirical R_c scaling relationships developed by HA67, used for the Mueller and Murphy (1971) model, and DJ91. These TOCs were obtained from an analysis of m_b and moment magnitude (M_w), while accounting for possible m_b bias and the effects of source medium elastic properties at the DPRK test site (Patton, 2011). Both

scaling relations are consistent with the measurements. The ambiguity over R_c scaling and the burial depth for this test translates into growing yield uncertainty as DoB increases.

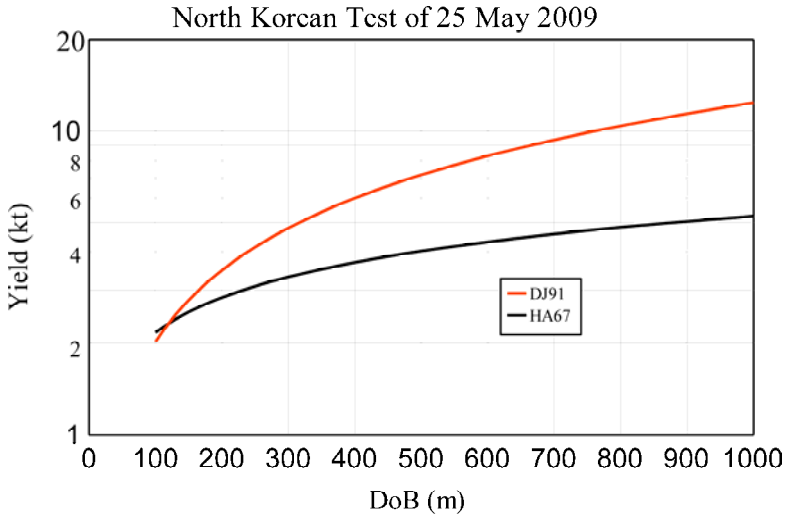

Figure 1. Yield : DoB tradeoff curves for the North Korean 2009 test (after Patton, 2011). Tradeoff curves based on HA67 and DJ91 R_c scaling equations are shown with black and red lines, respectively.

Non-linear material responses and strong-motion phenomenology of the source medium control R_c evolution and play a significant role in seismic-wave generation of buried explosions. Nuclear testing was dominated by standard containment practices. As such, much better agreement is seen between R_c scaling models for SDoB consistent with these practices. Due to limited R_c data for non-standard burial depths, hydrodynamic computations involving realistic material response models offer a viable alternative to answering questions about R_c evolution and statics. In this paper, such questions are investigated through a series of computations for a granite medium. The results will test the veracity of R_c scaling models and will even help constrain the SDoB of the 2009 DPRK test.

Hydrodynamic Modeling in Granite. A wide range of physical and thermodynamic phenomena control shock wave propagation for underground nuclear explosions. Four different phenomenological zones can be identified according to the material behavior. The first zone, usually called the source region, is where the rock and device material are vaporized due to the huge amount of energy released from the explosion. As the shock wave propagates outward, the energy dissipates due to mechanical and geometric factors. At a certain range the amount of energy is no longer sufficient to vaporize the rock but is sufficient to melt it in a second zone called the cavity region. As the shock wave propagates further, the rock material no longer melts, but it undergoes significant irreversible deformations and fracturing. This defines a third zone called the permanently deformed region. The material starts to behave elastically at a radius roughly an order of magnitude larger that R_c, therefore defining the fourth zone called the elastic region. In the numerical results R_c is considered to be the radius that defines the boundary between the second and the third phenomenological zones.

To properly account for wave propagation across all the zones and also for the correct energy deposition in the elastic zone, a series of key design constraints are identified. These constraints are obtained from the available experimental data for Hardhat and Piledriver explosions detonated in granite on Climax Stock of the Nevada Test Site, (Rimer et al., 1990; Murphy, 1978; Antoun et al., 2001; Perret and Bass, 1974), and are to be employed as design parameters for the purpose of developing an appropriate material model. The constraints selected are: (1) velocity and displacement waveforms, (2) energy partition for each zone defined above, (3) peak velocity attenuation profiles and (4) R_c.

The three most common approaches for modeling the source region are: iron gas model, bubble model with ideal gas, and bubble model with tabulated equation of state (EOS). The bubble model considers that the energy of the explosion is uniformly distributed over a vaporization sphere with radius in meters, $R_v \approx 2.0\ W^{1/3}$, Schroeder (1974), where W is the yield of the explosion measured in kilotons. The iron gas model assumes that after the explosion an

iron gas is formed occupying a spherical region around the shot point. The initial energy of the explosion is uniformly distributed over this spherical region, which has a radius smaller than R_v. Different material models have been used in the past to describe the behavior of the "bubble" or source region. The two most common material models employed for this purpose are: ideal gas with a density equal to the density of the rock under consideration (Antoun et al., 2001), and a tabular EOS, i.e., Sesame tabular EOS (Abdallah et al., 1980).

The three approaches for modeling the source region were tested against Hardhat and Piledriver observations, and none satisfied all of the design constraints. The results for the bubble model with an ideal gas matched constraints #1 and #3, but over predicted #4 and the energy distribution #2 was not realistic. After the shot, a very small amount of the total energy (around 4%) was in the source region, while in reality at least 30% of the energy released is needed just to vaporize the granite contained within R_v. The iron pill and bubble models with the Sesame EOS gave reasonably good results for #4 and energy distribution #2, but both under predicted #1 and #3. These EOS models do not fully account for the first principle physics of shock wave continuum from the cavity expansion to final energy deposition.

The importance of correct energy deposition and cavity dynamics required finding a different EOS model for granite media. Tillotson (1962) introduced a dependency on the specific internal energy of the material and accounted for phase changes from solid to vapor. A series of parameters, based on a modified version due to Melosh (1989), are used to describe the behavior of the material across the different phases. The source modeling was then accomplished by coupling the Tillotson EOS with the bubble model.

The material model is completed by combining the EOS with an appropriate strength model. The main component of the strength model for granite is the "yield surface", which describes how the shear strength changes with confinement pressure. The adopted undamaged yield surface ($Y_{undamage}$) was derived from Fossum and Brannon (2004), where modifications were introduced to match the field data for Hardhat and Piledriver.

The material model also incorporates a shear strain softening behavior, which follows the one presented by Rubin et al. (2000). The undamaged yield surface curve is scaled down as a function of the strain softening factor (f_{soft}) as follows

$$Y = Y_{undamage}\, f_{soft} \quad ; \quad f_{soft} = 1 - a\ \exp\left(- \frac{b\,(1-\Omega)^2}{\Omega} \right) \tag{1}$$

where f_{soft} is the softening factor, a and b are material fitting constants, and $\Omega = \min\left(\varepsilon_p / \varepsilon_d, 1\right)$ is the shear damage, where ε_p is the plastic shear strain and ε_d is the value of the plastic shear strain for which the damage is maximum, i.e. Ω is one and therefore $f_{soft} = 1 - a$.

Experimental data from Hardhat and Piledriver explosions were used as a reference for adjusting the material model parameters. Much work has been done in the past to simulate these two explosions with different material models (Antoun et al., 2001; Stevens et al., 2000; Stevens et al., 2001). However, to the authors' knowledge, constraint #2 is yet to be reported in this kind of study. In the following section, the objective of satisfying all design constraints is accomplished using the modeling approach just described for 1-D simulations.

Fits to freefield ground motion, energy distribution and R_c. Figure 2 shows a comparison of the calculated against the observed free field velocity waveforms for the Hardhat event as a function of time.

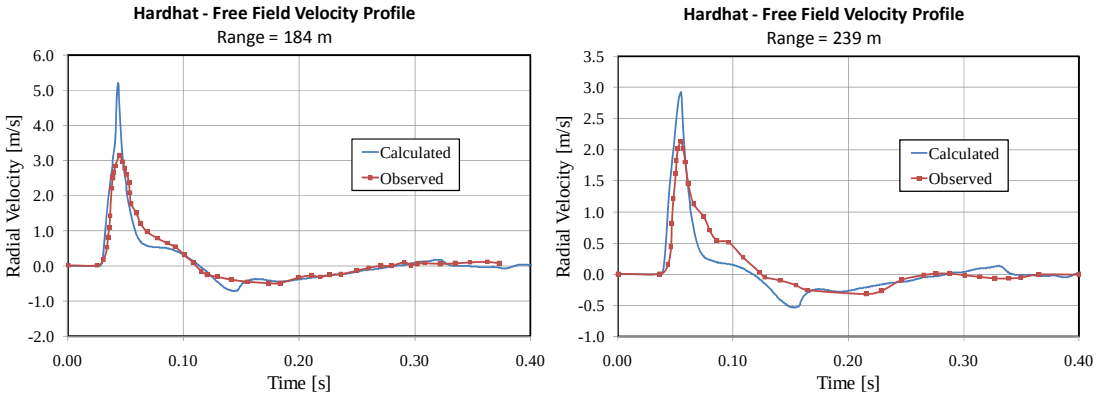

Figure 2. Material model validation: HARDHAT: Comparison of calculated vs. observed velocity profiles for different ranges. The calculated velocity profiles were obtained using the material model with just strain softening behavior.

At the end of the Hardhat simulation the energy distribution per zone was: zone 1: 46%, zones 2 and 3: 50%, and zone 4: 4%. The amount of energy deposited in zone 4 gives the seismic efficiency of the underground nuclear explosion which compares favorably with 1.8% for the granite shot Shoal reported by Mueller (1969). This high energy value obtained from the Hardhat simulation and the slight over-estimation of peak velocities on Figure 2 can be explained by the fact that many dissipative factors are not currently considered in the computational model, such as pre-existing faults and fractures.

As the energy propagates across the computational model a certain amount of work due to compression is done on the cells of the model. This work, which is essentially given by $p\ dv$, where dv is the volume change, increases the specific internal energy of the cell, therefore increasing its temperature. When the specific internal energy reaches a given value, the material starts to melt. The position of the last melted cell from the center of the source was the criterion used to identify where the boundary of the cavity area is located. The calculated and measured values of R_c for Piledriver are 39.4 and 44.5 respectively and for Hardhat are 17.9 and 19.4 m. Differences between calculated and measured R_c of only 11.5% and 7.7% respectively are indication of fairly good agreement. It is worth noting that the predictions of HA67 and DJ91 for Hardhat are 21.4 and 18.4 m respectively.

Effects of Scaled Depth of Burial. In this section, the effects of over-burden on R_c evolution and on material damage for a 2-D axially symmetric computational model are investigated utilizing the material models discussed above. A 1-kt source is placed at different DoB (125, 250, 500 and 1000 m) in a homogeneous granite medium with Young modulus: 70.22 GPa, density: 2680 kg/m^3 and Poisson ratio: 0.226 (P-wave velocity: 5495 m/s, S-wave velocity: 3269 m/s). The free surface is flat, i.e. no topography. The influence of the gravitational field is taken into account in the model, i.e. a lithostatic stress state is prescribed as an initial condition.

The final value of R_c is recorded for each DoB and compared to the predictions of scaling relationships due to HA67 and DJ91 as shown in Figure 3. Plotted is HA67's empirical scaling equation for R_c, the same as equation (19) in Mueller and Murphy (1971), and equation (39) of DJ91. The scaling equations show good agreement for SDoB near 120 m/kt$^{1/3}$. Most R_c measurements on which the empirical scaling equations were based are for explosions detonated at these nominal containment depths. Far fewer measurements were available for large SDoB where the predictions steadily diverge to the point that they differ by 51% (11.2 versus 7.4 m) at 1000 m/kt$^{1/3}$. The numerical results are in much better agreement with DJ91's scaling equation, even for quite deeply buried events.

Another effect of SDoB is the amount of permanent damage due to shock wave interactions with the free surface. Figure 4 shows shear damage profiles for different SDoBs. At a nominal SDoB, there is a substantial amount of shear damage on the free surface, while damage decreases as SDoB increases, as expected. It can be inferred that a SDoB of 209 m/kt$^{1/3}$ is the limit where almost no shear damage is noticeable for a uniform granite medium with material properties specified above and a flat free surface. It is worth noting that extensive free surface damage (up to a range of 753 m) in the form of spallation was observed for the Piledriver event, (Bache, 1976).

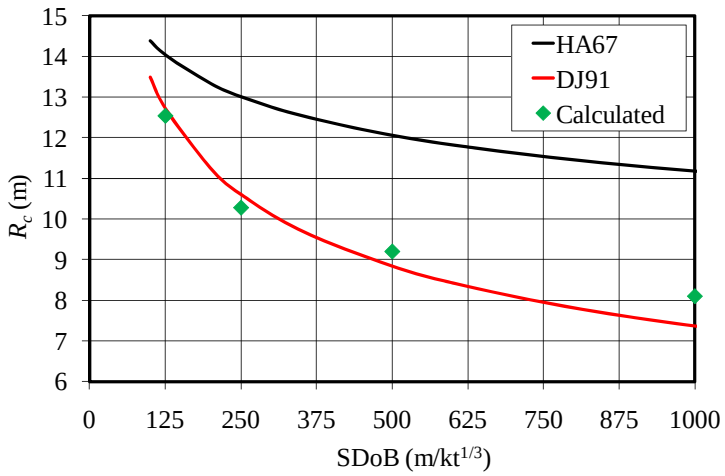

Figure 3. Cavity radius, Rc, as a function of SDoB for a 1 kt explosion in granite.

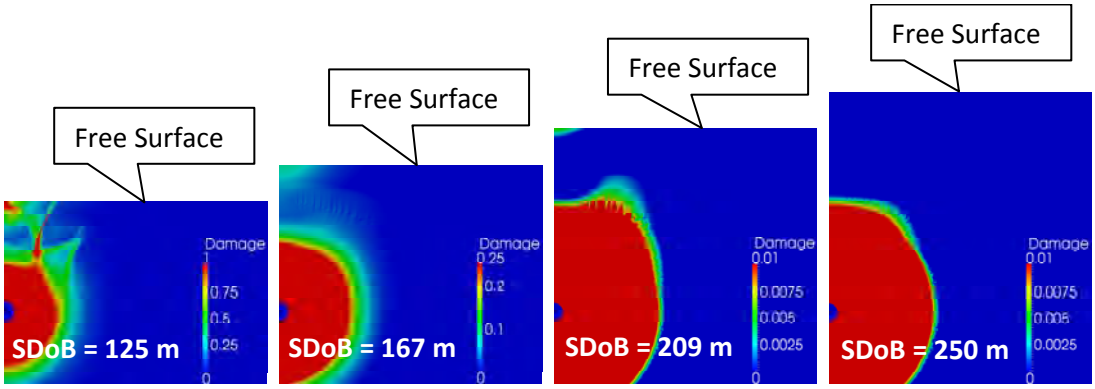

Figure 4. Shear damage for different SDoBs. Yield = 1.0 kt.

Material Model Enhancements. As part of the ongoing research effort the material model developed last year was enhanced by incorporating shear hardening on top of the already implemented shear softening behavior. The hardening process adopted in this work is described in detail by Rubin et al. (2000). The working yield surface is then obtained as follows

$$Y = Y_{undamage}\, f_{soft}\, f_{hard} \tag{2}$$

where $Y_{undamage}$ is the yield surface of the intact material, f_{soft} is given by equation (1) and f_{hard} is the hardening factor which is given by

$$f_{hard} = c + (1-c)\exp(-\varepsilon_p d) \tag{3}$$

where c is the amount of hardening for the material, ε_p is the equivalent plastic strain and d is a parameter that defines how fast the shear hardening is applied as a function of ε_p. With the introduction of the hardening factor the response of the material as it undergoes plastic deformation in shear can be divided into two phases: in the first phase the material hardens until it reaches maximum shear strength. As the equivalent plastic strain grows softening behavior starts to be more preponderant than the hardening and therefore the shear strength degrades up to a defined minimum as shown in Figure 5a. In Figure 5b the corresponding yield surfaces are shown.

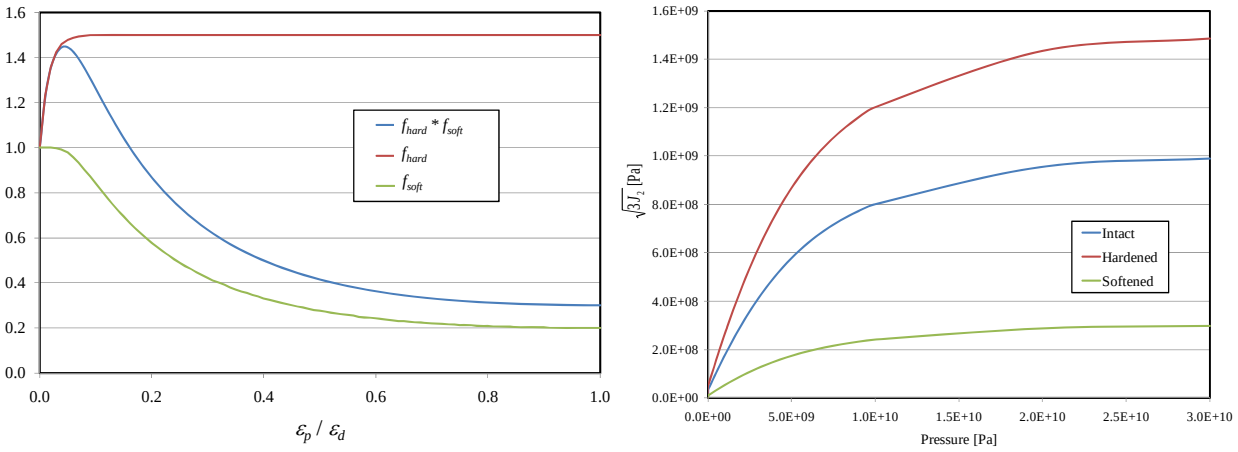

a) **b)**

Figure 5. a) Softening and hardening factors as a function of the equivalent plastic strain. b) Yield surfaces utilized in the improved material model.

In order to adjust this newly developed material model a set of numerical simulations were conducted for the Hardhat event. The results obtained for the radial velocity waveforms at ranges 184 m and 239 m are shown in Figure 6. The matching between the calculated results and the observed values is excellent and the improvement can be readily appreciated (see Figure 2). The final cavity radius obtained from the simulations was 19.0 m, which is in much closer agreement (2% difference with the measured value, 19.4 m) than the results obtained using the material model developed last year, 17.9 m.

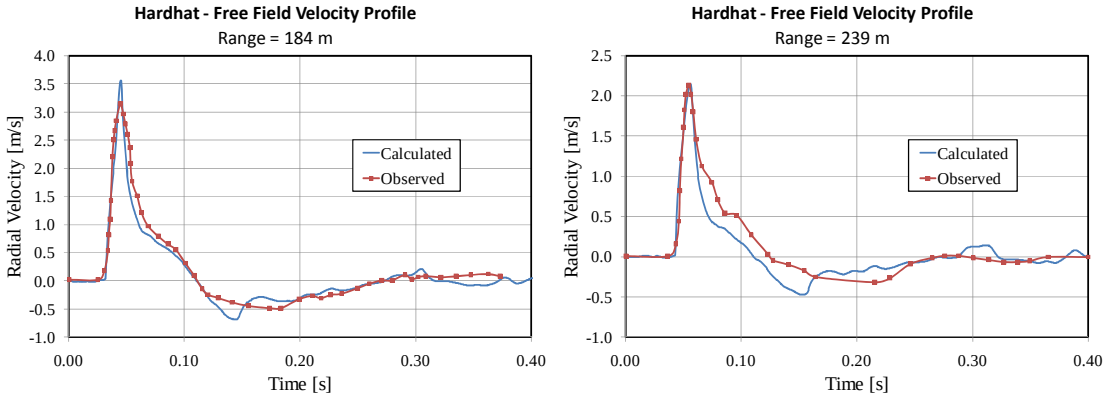

Figure 6. HARDHAT: Comparison of calculated vs. observed velocity profiles for different ranges. The calculated velocity profiles were obtained using the improved material model (with strain hardening and softening behavior).

CONCLUSIONS AND RECOMMENDATIONS

A lower yield limit for the 2009 North Korean test can be established by combining the above results with the TOCs discussed in earlier in the paper. Satellite images of the 2006 and 2009 tests showed no evidence of free surface disturbances caused by spallation (Schlittenhardt et al., 2010; Begnaud et al., 2011). Figure 7 shows curves of constant SDoB corresponding to 125, 209 and 250 m/kt$^{1/3}$ plotted with the TOCs. The curve for 209 m/kt$^{1/3}$ is the calculated estimate of the threshold for shear damage expected at the free surface for an explosion in granite: i.e., if the explosion was buried much shallower than 209 m/kt$^{1/3}$, the effects of spallation and free surface damage should have been great enough to be noticed from satellite imagery. This constraint means that a combination of DoB and yield should be located to the right of this curve. Since the numerical results favor the R_c scaling equation of DJ91

over HA67 (Figure 3), estimates of the minimum DoB and yield for the 2009 DPRK test are 375 m and 5.7 kt, respectively. Greater DoB and larger yields should follow the trajectory defined by the DJ91 TOC curve.

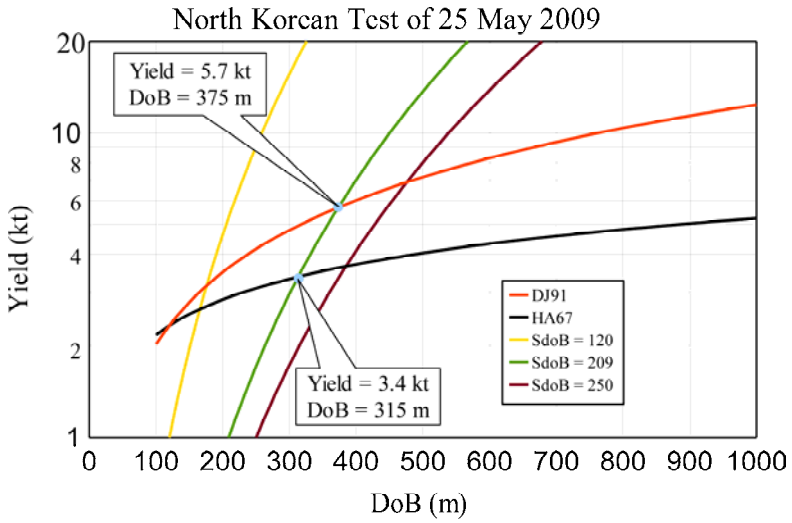

Figure 7. Yield vs. DoB tradeoff curves for the North Korean 2009 test (after Patton, 2011). Tradeoff curves based on HA67 and DJ91 R_c scaling equations are shown with black and red lines, respectively. Trajectories of constant SDoB are shown by yellow, green, and brown lines.

In summary, hydrodynamic simulations play an important role in investigating the effects of non-linear material response and strong-motion phenomenology on R_c scaling and seismic-wave generation for source emplacements with limited experience or data from past nuclear tests. The focus of this study was to predict final R_c for explosions detonated in a granite medium and to determine a threshold for permanent damage on the free surface as SDoB increases. The results agree with the empirical R_c scaling model of DJ91 and, along with a previously developed yield : DoB tradeoff curve, constrain lower bounds on the yield and DoB of the 25 May 2009 DPRK test.

3D Topographic Effects. Refined 3D simulations including surface topography, complex structures and morphology will be conducted to augment the understanding of R_c scaling and seismic-wave generation for realistic explosion source regions. The first stage of this next step will be to develop a computational model taking into account the topography of the Nevada National Security Site (NNSS) area 15-b (Figure 8) and to investigate the effects of introducing topography on the generation of shear waves. Preliminary results will be presented at the conference.

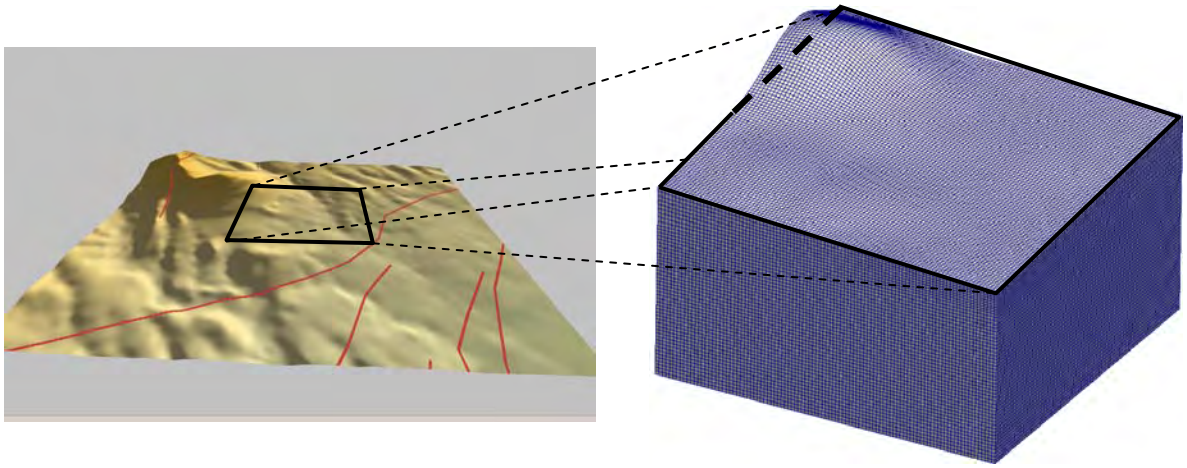

Figure 8. Left: Digitized Elevation Map of the NNSS Area U-15b. Right: Finite volume model with topography.

Near to Far Field Propagation. As part of this year's efforts we have begun the process of coupling the hydrodynamics output to a far field seismic wavefield propagation code SPECFEM3D. SPECFEM3D is a spectral element code that allows for complex topography, full othorhombic anisotropy and intrinsic attenuation (Komatitsch, 1997; Komatitsch and Vilotte, 1998). Our current model has the topography of Area 15 at the Nevada National Security Site and a two layer model of the weathered and intact Climax Stock granodiorite. Careful analysis of the shear wave field generated near source will be compared with that generated in the far field.

The above analysis can then be followed with the development of a computational model that considers the real topography of the North Korean test site (Figure 9). In so doing, further refinement of the minimum yield and depth of burial predicted earlier can be achieved.

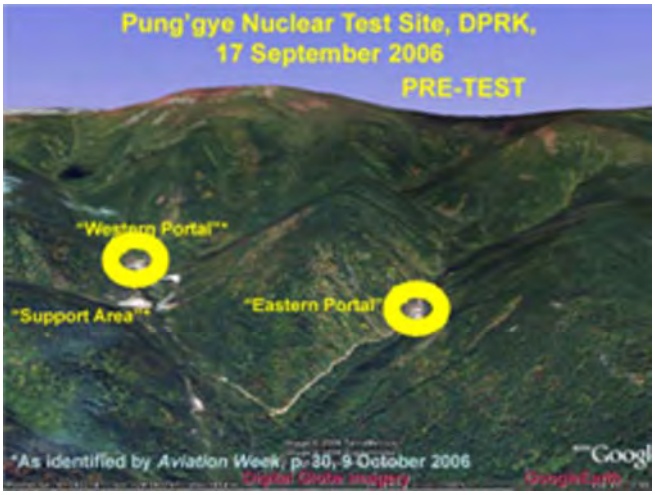

Figure 9. A photograph of the location of the East and West portals at the North Korean test site, Pung'gye, is shown.

ACKNOWLEDGEMENTS

Part of the material presented in this paper has been accepted for publication in the Geophysical Research Letters (Geophys. Res. Lett., doi:10.1029/2011GL048269, in press.). We would like to thank the anonymous reviewer of that paper for helpful comments. Thanks to our colleagues and collaborators for the support and the advice provided during this project. Special thanks to our colleagues Dr. Thomas N. Dey and Dr. Hans E. Hartse for providing their valuable comments on the paper to be published.

REFERENCES

Abdallah, J. Jr., G. I. Kerley, B, I. Bennett, J. D. Johnson, R. C. Albers and W. F. Huebner (1980). HYDSES: a subroutine package for using SESAME in hydrodynamic codes, Los Alamos Scientific Laboratory Report LA-8209.

Antoun, T. H., I. N. Lomov, and L. A. Glenn (2001). Development and application of a strength and damage model for rock under dynamic loading, The 38th U.S. Rock Mechanics Symposium, UCRL-JC-142748.

Bache, T. C. (1976). The effects of tectonic stress release on explosion P-wave signatures, *Bull. Seismol. Soc. Am*, 66(5): 1441–1457.

Begnaud, M. L., W. S. Phillips, R. J. Stead, and F. V. Pabian (2011). (U) Constraints on the locations of the 2009 and 2006 DPRK P'unggye explosions from fusion of improved relative relocation and geospatial analysis, Defense Research Review, (classified) 19.1, 1-16 (NSI/NOFORN).

Denny, M. D. and L. R. Johnson (1991). The explosion seismic source function: models and scaling laws reviewed, *Explosion source phenomenology. Geophysical monograph 65,* American Geophysical Union: 1–24.

Douglas, A. and P.D. Marshall (1996). Seismic source size and yield for nuclear explosions, in Monitoring a Comprehensive Test Ban Treaty, NATO ASI Series, Series E, 303, 309-353.

Fossum A. F. and R. M. Brannon (2004) THE SANDIA GEOMODEL: Theory and User's Guide. Sandia National Laboratories.

Heard, H. C. and F. J. Ackerman (1967). (U) Prediction of cavity radius from underground nuclear explosions, Lawrence Radiation Laboratory Report, UCRL-50324.

Komatitsch, D. (1997) Méthodes spectrales et éléments spectraux pour l'équation de l'élastodynamique 2D et 3D en milieu hétérogène (Spectral and spectral-element methods for the 2D and 3D elastodynamics equations in heterogeneous media). PhD thesis, Institut de Physique du Globe, Paris, France. 187 pages.

Komatitsch, D. and J. P. Vilotte (1998). The spectral-element method: an efficient tool to simulate the seismic response of 2D and 3D geological structures. *Bull. Seismol. Soc. Am.*, 88(2):368–392.

Melosh, H. J. (1989) Impact cratering. A geologic process. *Oxford Monographs on Geology and Geophysics:* 11.

Mueller, R. A. (1969). Seismic energy efficiency of underground nuclear detonations, *Bull. Seismol. Soc. Am*. 59, 2311-2323.

Mueller, R. A. and J. R. Murphy (1971). Seismic characteristics of underground nuclear detonations. Part I. Seismic spectrum scaling, *Bull. Seismol. Soc. Am.*, 61(6): 1675-1692.

Murphy, J. R. (1978). A review of available free-field seismic data from underground nuclear explosions in salt and granite, Interim Technical Report CSC-TR-78-0003.

Patton, H. J. (2011) A Method to Infer Material Properties and mb Bias of the North Korean Test Site Using Yield : Depth-of-Burial Tradeoff Curves and {mb − Ms} Double Differences. *Bull. Seismol. Soc. Am*. 101 in press, December publication.

Perret, W. R. and R. C. Bass (1974). Free-field ground motion induced by underground explosions, Sandia National Laboratory Report SAND74-0252.

Rimer, N., J. Stevens, and D. Halda (1990). Modeling of the ground motion from events in genetic rocks, *Modeling and Material Properties Working Group of the CAT*, SSS-DVR-90-11661.

Rubin, M. B., O. Y. Vorobiev and L. A. Glenn (2000). Mechanical and numerical modeling of a porous elastic-viscoplastic material with tensile failure, *Int. J. Solids Struct*, 37: 1841-1871.

Schlittenhardt, J., M. Canty, and I. Grünberg (2010). Satellite Earth observations support CTBT monitoring: A case study of the nuclear test in North Korea of Oct. 9, 2006 and comparison with seismic results, *Pure Appl. Geophys*. doi: 10.1007/s00024-009-0036-x.

Schroeder, R. C. (1974). A comparison of initial conditions for nuclear explosion calculations, UCRL-51671.

Stevens, J. L., N. Rimer, J. R. Murphy, H. Xu, G. G. Kocharyan and B. A. Ivanov (2000) Near field and regional modeling of explosions at the Degelen test site, in *Proceedings of the 22nd Annual DoD/DOE Seismic Research Symposium: Planning for Verification of and Compliance with the Comprehensive Nuclear-Test-Ban Treaty*, LA-UR-99-4700, Vol. 1.

Stevens, J. L., N. Rimer, H. Xu, J. R. Murphy, G. E. Baker, G. G. Kocharyan, B. A. Ivanov and S. M. Day (2001) Near field and regional modeling of explosions at the Degelen test site, in *Proceedings of the 23rd Seismic Research Review: Worldwide Monitoring of Nuclear Explosions*, LA-UR-01-4454, Vol. 1, pp. 540–549.

Tillotson, J. H. (1962). Metallic equation of state for hypervelocity impact, AF 29(601)-4759, ARPA Order 251-61.